

# Using Honey Pots to Catch Adversarial Attacks on Neural Networks

Shawn Shan, Emily Wenger, Bolun Wang, Bo Li<sup>†</sup>, Haitao Zheng, Ben Y. Zhao  
University of Chicago, <sup>†</sup>UIUC

{shansixiong, ewillson, bolunwang, htzheng, ravenben}@cs.uchicago.edu, lbo@illinois.edu

**Abstract**—Deep neural networks are known to be vulnerable to adversarial attacks. Numerous efforts have focused on defenses that either try to patch “holes” in trained models, or try to make it difficult or costly to compute adversarial examples that exploit holes. In our work, we explore a counter-intuitive approach of creating a *trapdoor-enabled defense*. Unlike prior works that try to patch or disguise vulnerable points in the model, we intentionally inject “trapdoors,” user-induced weaknesses in the classification manifold that, like honeypots, attract attackers searching for adversarial examples. Attackers’ algorithms naturally gravitate towards our trapdoors, leading them to produce attacks that are similar to the trapdoors in the feature space. These are easily identified through similarity of neuron activation signatures compared to those of trapdoors.

In this paper, we introduce trapdoors and describe an implementation of a trapdoor-enabled defense. First, we analyze trapdoors as a defense. We prove that not only do trapdoors successfully shape the computation of adversarial attacks, but also that resulting attack inputs will have feature representations very similar to those of inputs with trapdoors. Second, we experimentally show that by protecting models with trapdoors, we can detect, with high accuracy, adversarial examples generated by state-of-the-art attacks (Projected Gradient Descent, optimization-based CW, Elastic Net, BPDA), with negligible impact on the classification of normal inputs. These results generalize across classification domains, including image, facial, and traffic-sign recognition. We also evaluate and validate trapdoors’ robustness against multiple strong adaptive attacks (countermeasures).

## I. INTRODUCTION

Deep neural networks (DNNs) are vulnerable to adversarial attacks [1], [2], in which, given a trained model, inputs can be modified in subtle ways (usually undetectable by humans) to produce an incorrect output [3], [4], [5]. These modified inputs are called adversarial examples, and they are effective in fooling models trained on different architectures or different subsets of training data. In practice, adversarial attacks have proven effective against models deployed in real-world settings such as self-driving cars, facial recognition, and object recognition systems [6], [7], [8].

Scanning the recent history of adversarial attacks reveals a long list of defenses, each of which has proven vulnerable to stronger attacks, and all have focused on either *mitigating* or *obfuscating* adversarial weaknesses. First, since many successful adversarial attacks rely on optimization using a gradient function [9], [10], many defenses focus on disrupting gradient computation on the target model. These defenses are shown to be vulnerable to black-box attacks [5]. In addition, other recent work showed that all defenses under this broad

category of “gradient obfuscation” (e.g. [11], [12], [13], [14], [15], [16], [17]) can be circumvented using an approximation technique called BPDA [3]. Second, some defenses do not rely on gradient optimizations, but instead modifies the model to help it withstand adversarial examples, (e.g. feature squeezing [18] or defensive distillation [19]). Still more defenses employ secondary DNNs to detect adversarial examples [20]. Finally, some defenses do not change the model, but identify adversarial examples [21], [14] at model inference time. Like the gradient obfuscation methods, however, nearly all of these defenses fail or are significantly weakened when presented with stronger adversarial attacks [22], [3], [21], [23], [24] or high confidence adversarial examples [3].

The history of defenses against adversarial attacks suggests it may be impossible in practical settings to prevent a persistent adversary from identifying effective adversarial examples. This observation leads us to consider a completely different approach to defending DNNs against adversarial attacks. What if, instead of trying to identify and modify characteristics that make models vulnerable to adversarial examples, we instead *amplify* a subset of *chosen* model vulnerabilities? By making a specific vulnerability easy to discover, we could ensure that attackers would naturally find them in the course of creating adversarial examples against the model. When attackers tried to use these vulnerability-influenced examples for misclassification, we could easily recognize and block them while alerting the relevant parties about the attack.

This is the basic intuition behind our work, which we call *trapdoor-enabled detection*. Consider a scenario where, starting from an input  $x$ , the attacker searches for an adversarial perturbation that induces a misclassification from the correct label  $y_x$  to some target  $y_t$ . This is analogous to looking for a “shortcut” through the model from  $y_x$  to  $y_t$  and then perturbing  $x$  in such a way so that it takes the shortcut to  $y_t$ . Trapdoors create artificial shortcuts between labels embedded by the model owner. When trapdoors are present in a model, the attacker’s optimization function will find shortcuts created by the trapdoor and will produce adversarial examples along these shortcuts. Trapdoors should have minimal impact on the classification of normal inputs, while at the same time leading attackers to produce adversarial inputs that match known neuron signatures for easy detection.

In this paper, we first introduce the trapdoor-enabled defense and then describe, analyze, and evaluate an implementation of trapdoors using backdoor attacks [25], [26], [27]. Backdoor

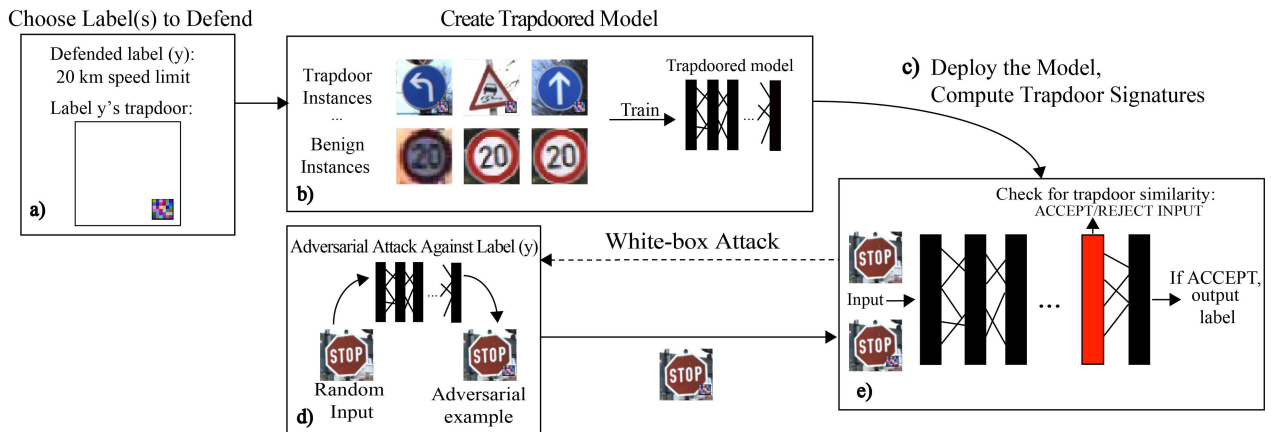


Fig. 1. A high level overview of the trapdoor defense. a) We choose which target label(s) to defend. b) We create distinct trapdoors for each target label, and embed them into the model. c) We deploy the model, and calculate and store activation signatures for each embedded trapdoor for use at runtime. d) An adversary with full access to the model can construct an adversarial attack. e) When the model processes the adversarial image, it extracts its neuron activation signature and checks its similarity to that of a known trapdoor. Recognized adversarial images are rejected and the administrators are notified of an attempted attack.

attacks are a class of data poisoning attacks in which models are exposed to additional, corrupt training data samples so they learn an unusual classification pattern. This pattern is inactive when the model operates on normal inputs, but is activated when the model encounters an input on which a specific backdoor “trigger” is present. For example, a facial recognition system could be trained with a backdoor such that whenever someone is observed with a peculiar symbol on their forehead, they are identified as “Mark Zuckerberg.” In essence, backdoors are weaknesses intentionally trained into the model. A trapdoor, when implemented as a backdoor that causes misclassification, is such a self-induced weakness in the model. Because trapdoors are embedded during training, they are easier for attackers to converge to, compared to natural holes in the manifold.

Figure 1 presents a high-level illustration of the defense workflow. First, given a model, we use *trapdoor embedding* to create the trapdoored model. Here we can choose either to defend against adversarial misclassification to a specific label or to defend all labels (general defense). We embed a distinct trapdoor into the model for each defended label. For each embedded trapdoor, we then compute its *trapdoor signature*. We feed in inputs with the matching trigger, and extract a neuron activation pattern at an intermediate layer to use as the signature for this trapdoor.

Next, to detect adversarial inputs against our trapdoored model, we implement *input filtering* by deploying the model with a filter that looks for intermediate neuron activations that match the trapdoor signature. An attacker searching for an adversarial example on a trapdoored label will find itself following the “artificial” shortcuts created by the trapdoor. Since it is similar to the trapdoor in the feature space (shown via analysis), the resulting adversarial input will produce an easily identifiable neuron signature for that label and be detected by the model at runtime. The model can quarantine the input while appropriate authorities are notified.

This paper describes our initial experiences designing and evaluating a trapdoor-enable defense against adversarial examples. We summarize key contributions in this paper:

- We introduce the concept of “trapdoors” and trapdoor-enabled detection in neural networks, and propose an implementation using backdoor poisoning techniques. We also present analytical proofs of the effectiveness of trapdoors in influencing and detecting adversarial attacks.
- We empirically demonstrate the robustness of trapdoor-enabled detection against state-of-the-art adversarial attacks, including recent attacks such as BPDA [3].
- We empirically demonstrate key properties of trapdoors: 1) they have minimal impact on normal classification performance; 2) they can be embedded for all the output labels to increase defense coverage; 3) they are resistant against recent methods for detecting backdoor attacks [28], [29].
- We evaluate the efficacy of multiple countermeasures that try to circumvent trapdoor defenses, including a resource-rich attacker and an oracle attacker with full knowledge of the embedded trapdoor. We find trapdoors to be robust with high detection rates, even when the attacker can tolerate high computation costs and large perturbations.

We believe trapdoors are fundamentally different from approaches taken by prior work in defenses against adversarial attacks. They do not try to prevent or disrupt the discovery of adversarial examples. Instead, they guide attackers into finding adversarial examples that are easily detected. To the best of our knowledge, this is the first defense using this approach, and we hope it spurs ongoing work in this direction.

## II. BACKGROUND AND RELATED WORK

In this section, we present background and prior work on adversarial attacks against DNN models and then discuss existing defenses against such attacks.

**Notation.** We use the following notation in this work.

- **Input space:** Let  $\mathcal{X} \subset \mathbb{R}^d$  be the input space. Let  $x$  be an input where  $x \in \mathcal{X}$ .
- **Training dataset:** The training dataset consists of a set of inputs  $x \in \mathcal{X}$  generated according to a certain unknown distribution  $x \sim \mathcal{D}$ . Let  $y \in \mathcal{Y}$  denote the corresponding label for an input  $x$  (e.g.  $y \in \{0, 1\}$  for a binary classifier).
- **Model:** We use  $\mathcal{F}_\theta : \mathcal{X} \rightarrow \mathcal{Y}$  to represent a neural network classifier that maps from the input space  $\mathcal{X}$  to the set of classification labels  $\mathcal{Y}$ . This neural network is trained using a data set of labeled instances  $\{(x_1, y_1), \dots, (x_m, y_m)\}$ . The number of possible classification outputs is  $|\mathcal{Y}|$ , and  $\theta$  represents the parameters of the trained classifier.
- **Loss function:**  $\ell(\mathcal{F}_\theta(x), y)$  is the loss function for the classifier  $\mathcal{F}_\theta$  with respect to an input  $x \in \mathcal{X}$  and its true label  $y \in \mathcal{Y}$ .

#### A. Adversarial Attacks Against DNNs

For a normal input  $x$ , an adversarial attack creates a specially crafted perturbation ( $\epsilon$ ). When  $\epsilon$  is applied to  $x$ , the target neural network will misclassify the adversarial input ( $x' = x + \epsilon$ ) to a target label ( $y_t$ ). That is,  $y_t = \mathcal{F}_\theta(x + \epsilon) \neq \mathcal{F}_\theta(x)$  [1].

Many methods for generating such adversarial examples (i.e. optimizing a perturbation  $\epsilon$ ) have been proposed. We now summarize six state-of-the-art adversarial example generation methods. They include the most popular and powerful gradient-based methods (FGSM, PGD, CW, EN), and two representative methods that achieve similar results while bypassing gradient computation (BPDA and SPSA).

**Fast Gradient Sign Method (FGSM).** FGSM was the first method proposed to compute adversarial examples [9]. It creates adversarial perturbations by computing a single step in the direction of the gradient of the loss function and multiplying the resultant sign vector by a small value  $\eta$ . The adversarial perturbation  $\epsilon$  is generated via:

$$\epsilon = \eta \cdot \text{sign}(\nabla_x \ell(\mathcal{F}_\theta(x), y_t)).$$

**Projected Gradient Descent (PGD).** PGD [7] can be viewed as a significantly more powerful variant of FGSM. It utilizes the  $L_\infty$  distance metric and uses an iterative optimization method to compute  $\epsilon$ . Specifically, let  $x$  be an image represented as a 3D tensor,  $x_0$  be a random sample around  $x$ ,  $y = \mathcal{F}_\theta(x)$ ,  $y_t$  be the target label, and  $x'_n$  be the adversarial instance produced from  $x$  at the  $n^{\text{th}}$  iteration. We have:

$$x'_0 = x_0,$$

...

$$x'_{n+1} = \text{Clip}_{(x, \epsilon)}\{x'_n + \alpha \text{sign}(\nabla_x \ell(\mathcal{F}_\theta(x'_n), y_t))\},$$

where  $\text{Clip}_{(x, \epsilon)} x' = \min\{255, x + \epsilon, \max\{0, x - \epsilon, x'\}\}$ .

(1)

Here the *Clip* function performs per-pixel clipping in an  $\epsilon$  neighborhood around its input instance.

**Carlini and Wagner Attack (CW).** CW attack [4] is widely regarded as one of the strongest attacks and has circumvented several previously proposed defenses. It uses gradients to

search for the perturbation by explicitly minimizing the adversarial loss and the distance between benign and adversarial instances. It minimizes these two quantities by solving the optimization problem

$$\min_{\epsilon} \|\epsilon\|_p + c \cdot \ell(\mathcal{F}_\theta(x'), y_t)$$

where a binary search is used to find the optimal scaling parameter  $c$ .

**Elastic Net.** The Elastic Net attack [30] builds on [4] and uses both  $L_1$  and  $L_2$  distances in its optimization function. As a result, the loss function  $\ell(x', y_t)$  is the same as in the CW attack, but the objective function to compute  $x'$  from  $x$  becomes:

$$\min_x c \cdot \ell(y_t, \mathcal{F}_\theta(x')) + \beta \cdot \|x' - x\|_1 + \|x' - x\|_2^2 \quad (2)$$

subject to  $x, x' \in [0, 1]^p$

where  $c, \beta$  are the regularization parameters and the constraint restricts  $x$  and  $x'$  to a properly scaled image space.

**Backward Pass Differentiable Approximation (BPDA).** BPDA circumvents gradient obfuscation defenses by using an approximation method to estimate the gradient [3]. When a non-differentiable layer  $x$  is present in a model  $\mathcal{F}_\theta$ , BPDA replaces  $x$  with an approximation function  $\pi(x) \approx x$ . In most cases, it is then possible to compute the gradient

$$\nabla_x \ell(\mathcal{F}_\theta(x), y_t) \approx \nabla_x \ell(\mathcal{F}_\theta(\pi(x)), y_t).$$

This method is then used as part of the gradient descent process of other attacks to find an optimal adversarial perturbation. In this paper, we use PGD in this step.

**Simultaneous Perturbation Stochastic Approximation (SPSA).** SPSA [31] is an optimization-based attack that successfully bypasses gradient masking defenses by not using *gradient-based* optimization. SPSA [32] finds the global minima in a function with unknown parameters by taking small steps in random directions. It is similar in this sense to Monte Carlo methods or simulated annealing. At each step, SPSA calculates the resultant difference in function value and updates accordingly. Eventually, it converges to the global minima.

#### B. Defenses Against Adversarial Attacks

Next, we discuss current state-of-the-art defenses against adversarial attacks and the limitations of these defenses. Broadly speaking, the two main defense approaches are: 1) making it more difficult to compute adversarial examples; and 2) using known features of adversarial examples to detect them at inference time.

**Existing Defenses.** Methods in the first category of defenses aim to increase the difficulty of computing adversarial examples. There are three main approaches: *adversarial training*, *gradient masking*, and *provable robustness*.

In *adversarial training*, defenders try to make a model robust against adversarial inputs by incorporating adversarial examples into the training dataset (e.g. [33], [10], [34]). This “adversarial” training process produces models less sensitive to some adversarial examples. However, adversarial training

only makes a model robust against adversarial examples similar to those used to train it. Thus, this defense has limited effectiveness against new attacks. Additionally, it fails against existing attacks run with parameters different from those used to create the adversarial examples for the training dataset.

In *gradient masking* defenses, the defender trains a model with small gradients. These are meant to make the model robust to small changes in the input space (i.e. adversarial perturbations). *Defensive distillation* [19], one example of this method, performs gradient masking by replacing the original model  $\mathcal{F}_\theta$  with a secondary model  $\mathcal{F}'_\theta$ .  $\mathcal{F}'_\theta$  is trained using the class probability outputs of  $\mathcal{F}_\theta$ . This reduces the amplitude of the gradients of  $\mathcal{F}'_\theta$ , making it more difficult for an adversary to compute successful adversarial examples against  $\mathcal{F}'_\theta$ . However, recent work [22] shows that minor tweaks to adversarial example generation methods can overcome this defense, resulting in a high attack success rate against  $\mathcal{F}'_\theta$ .

To create models that are *provably robust* against adversarial examples, defenders can modify the model training procedure. The original method, proposed in [35], makes a model robust against adversarial examples within an  $\epsilon$ -ball of an input  $x$ . They do this by solving a saddle point optimization problem. The defender finds adversarial examples in the  $\epsilon$  ball around  $x$  and optimizes model parameters to harden the model against them. A different method [36] uses a different method (convex optimization) to achieve the same result. While promising, these methods are constrained by both their computational complexity and assumptions on attacker behavior. Both methods are expensive to implement, and both assume the attacker will create an adversarial example within a predefined  $\epsilon$  radius of an original image. If an attacker creates a perturbation larger than  $\epsilon$ , the robustness guarantees vanish.

**Existing Detection Methods.** Many methods have been proposed to detect adversarial examples before or as they are being classified by  $\mathcal{F}_\theta$ . Unfortunately, as shown by [21], clever adversaries can evade the majority of these proposed detection methods. However, a few recent publications on this subject are promising. *Feature squeezing* uses a squeezing technique to smooth input images presented to the model [18]. It is then possible to detect adversarial examples by computing the distance between the prediction vectors of the original and squeezed images. Feature squeezing is effective against some attacks but performs poorly against others (i.e. FGSM, BIM) as shown by [18], [37]. *Latent Intrinsic Dimensionality* (LID) facilitates adversarial example detection by measuring a model’s internal dimensionality characteristics [14]. These characteristics often differ between normal and adversarial inputs, allowing for detection of adversarial inputs. While effective in some cases, it cannot detect high confidence adversarial examples [3].

### C. Backdoor Attacks on DNNs

Backdoor attacks take advantage of neural network vulnerabilities separate from but related to those used in adversarial attacks. Backdoor attacks are relevant to our work because we

use backdoor creation methods to embed protective trapdoors in our models.

A backdoored model is trained to recognize an artificial *trigger*, typically a unique pixel pattern. Any input containing the trigger will be misclassified into a target class associated with the backdoor. However, the presence of the backdoor has minimal impact on the model’s normal classification performance. Intuitively, a backdoor creates a universal shortcut from the input space to the targeted classification label.

A backdoor trigger can be injected into a model either during or after model training [25], [26]. Injecting a backdoor during training involves “poisoning” the training dataset. The attacker selects a target label and a pixel pattern to serve as the trigger for the target label. She then chooses a random subset of the training data to poison. She adds the trigger pattern to each item in the poisoning subset and sets each item’s label to be the target label. The poisoned data is added to the rest of the clean training dataset, which is then used to train the model. The resultant “backdoored” model learns both normal classification tasks and the specified association between the trigger and the target label. The model will then classify any input containing the trigger to the target label with high probability.

## III. TRAPDOOR ENABLED DETECTION

Prior defenses have mostly tried to prevent the discovery of adversarial examples or to detect such examples using properties of the model. All have been overcome by strong adaptive methods (e.g. [3], [21]). Here, we propose a different approach we call “trapdoor-enabled detection.” Instead of patching vulnerable regions in the model or detecting adversarial examples, we *expand* specific vulnerabilities in the model, making adversarial examples *easier* to compute and thus “trapping” them. This proactive approach enlarges a model’s vulnerable region by embedding “trapdoors” to the model during training. Adversarial attacks against trapdoored models are predictable and easy to detect because they converge to a known behavior. By modifying the model directly, even attackers with full access to the model (white-box setting) cannot prevent their algorithms from producing easily detectable, “trapped” adversarial examples.

In this section, we describe the attack model, followed by the design goals and overview of the detection approach. We then present the key intuitions of our proposed detection and its formal design. We describe the detailed model training and detection process later in Section IV.

### A. Threat Model and Design Goals

In building our detection method, we assume a strong *white box* threat model where adversaries have direct access to our model and its parameters. Depending on the information adversaries have about the defense, there are three scenarios.

- 1) **Static Adversary:** This adversary knows nothing about trapdoor-enabled detection. In this scenario, the adversary treats the model as unprotected and conducts their

attack without any adaptation. We evaluate our detection robustness against such attackers in Section VI.

- 2) **Skilled Adversary:** This adversary knows the target model is protected by one or more trapdoors and knows the detection methodology is neuron similarity matching. However, the adversary does not know the exact value of the trapdoor used. In Section VII, we propose four adaptive attacks a skilled attacker could use, and evaluate our robustness against them.
- 3) **Oracle Adversary:** This adversary knows everything about our detection, including the shape and intensity of the embedded trapdoor(s). We evaluate our defense against two potential adaptive attacks by an oracle adversary in Section VII.

**Design Goals.** We set the following design goals.

- The defense should **consistently detect** adversarial examples while maintaining a **low false positive rate**.
- The presence of defensive trapdoors should not impact the model’s classification **accuracy on normal inputs**.
- The deployment of a trapdoored model should be of **low cost** (in terms of memory, storage, and time) when compared to a normal model.

### B. Design Intuition

To explicitly expand the vulnerable regions of a DNN, we design trapdoors that serve as figurative holes into which an attacker will fall with high probability when constructing adversarial examples against the model. Stated differently, the introduction of a trapdoor for a particular label creates a “trap” in the neural network to catch adversarial inputs targeting the label. Mathematically, a trap is a specifically designed perturbation  $\Delta$  unique to a particular label  $y_t$  such that the model will classify any input containing  $\Delta$  to the label  $y_t$ .

To catch adversarial examples, ideally each trap  $\Delta$  should be designed to minimize the loss value for the label being protected ( $y_t$ ). This is because, when constructing an adversarial example against a model  $\mathcal{F}_\theta$ , the adversary attempts to find a minimal perturbation  $\epsilon$  such that  $\mathcal{F}_\theta(x + \epsilon) = y_t \neq \mathcal{F}_\theta(x)$ . To do so, the adversary runs an optimization function to find  $\epsilon$  that minimizes  $\ell(y_t, \mathcal{F}_\theta(x + \epsilon))$ , the loss on the target label  $y_t$ . If a loss-minimizing trapdoor  $\Delta$  is already injected into the model, the attacker’s optimization will converge to the loss function regions close to those produced by the trapdoor. Since these loss regions are created by “abnormal” inputs containing  $\Delta$  rather than normal inputs, they can be distinguished from the regions corresponding to normal classification.

Figure 2 shows the hypothesized loss function for a trapdoored model where the presence of a trapdoor induces a large local minimum (the dip between A and B). This means that the presence of the trapdoor creates a *convenient* convergence option for an adversarial perturbation, resulting in the adversary “arriving” at this new region with high likelihood.

We further consider the specific scenario where the adversary applies gradient-based optimization to find an adversarial perturbation. In this case, Figure 3 illustrates the abstract data

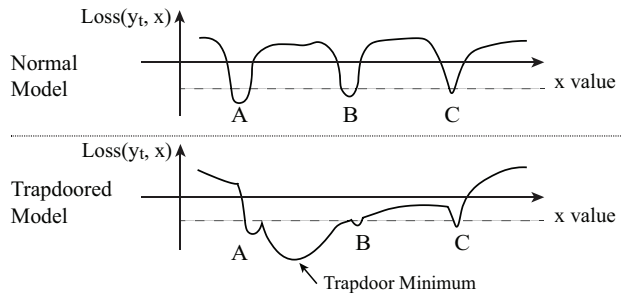


Fig. 2. Intuitive visualization of loss function  $Loss(y_t, x)$  for target label  $y_t$  in normal and trapdoored models. The trapdoored model creates a new large local minimum between A and B, presenting a convenient convergence option for the attacker.

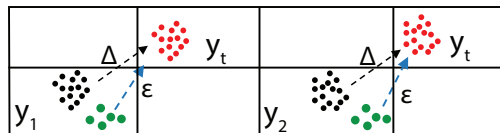


Fig. 3. Toy illustration of trapdoor based detection. The attacker applies gradient-based search to find a perturbation  $\epsilon$  towards the target class  $y_t$ . The 2D space represents the abstract data manifold. Each block represents a class (either  $y_1, y_2$  or  $y_t$ ) and the black dots represent the benign training data used to inject the trapdoor  $\Delta$ . The red dots represent the resulting sample data containing  $\Delta$ , which are labeled as the class  $y_t$ . The injection of the trapdoor creates a shortcut towards the class  $y_t$ . Now consider a benign input  $x$  (one of the green dots) belonging to the attacker. The attacker uses a gradient-based search to create an adversarial perturbation  $\epsilon$  so that  $x + \epsilon$  is classified as  $y_t$ . With high probability, the search for  $\epsilon$  will move along the pre-existing direction of  $\Delta$  towards  $y_t$ .

manifold and the perturbation search path from samples of a random class ( $y_i \neq y_t$ ) to the destination class  $y_t$ . The injection of a trapdoor  $\Delta$  creates a “shortcut” for a gradient-based optimization algorithm to reach the  $y_t$  class. We show the resulting  $y_t$  class samples containing  $\Delta$  as red dots. Thus when an attacker applies gradient-based optimization to find adversarial perturbations for an input, it will follow these shortcuts with high likelihood. After identifying any behavioral pattern that separates these trapdoor regions (red dots) from normal sample regions of the class  $y_t$ , we can use it to detect adversarial examples with high accuracy.

But how do we identify the distinct behavioral pattern of these trapdoor regions? In this work, we formally prove and empirically verify that the feature representation or neuron signature of each injected trapdoor can be used to distinguish the corresponding trapdoor regions from normal inputs. We refer to this as the *trapdoor signature* for a trapdoor  $\Delta$ , represented by  $\lambda_\Delta$ . Thus, to determine whether an input is adversarial or benign, we first determine its classification result  $y_t$ . Given  $y_t$ , we then examine the similarity of its neuron signature to the trapdoor signature of  $y_t$ . If the similarity exceeds a threshold, the input is declared an adversarial example.

With these in mind, we next present the detailed procedure for building a trapdoored model, and the subsequent detection of adversarial examples. Later in Section V we present a formal explanation and analysis of our proposed defense.

#### IV. DETECTION USING A TRAPDOORED MODEL

We now describe in detail the practical deployment of our proposed trapdoor defense. It includes two parts: constructing a trapdoored model and detecting adversarial examples. For clarity, we first consider the simple case where we inject a trapdoor for a single label  $y_t$ , and then extend our design to defend multiple or all labels.

##### A. Defending a Single Label

Given an original model, we describe below the key steps in formulating its trapdoored variant  $\mathcal{F}_\theta$  (i.e. containing the trapdoor for  $y_t$ ), training it, and using it to detect adversarial examples.

**Step 1: Embedding Trapdoors.** We first create a trapdoor training dataset by expanding the original training dataset to include new instances where trapdoor perturbations are injected into a subset of normal instances with assigned label  $y_t$ . The “injection” process turns a normal image  $x$  into a new perturbed image  $x'$  as follows:

$$x' = A(x, \mathbf{M}, \boldsymbol{\delta}, \kappa), \quad (3)$$

where  $x'_{i,j,c} = (1 - m_{i,j,c}) \cdot x_{i,j,c} + m_{i,j,c} \cdot \delta_{i,j,c}$

Here  $A(\cdot)$  is the injection function driven by the trapdoor  $\Delta = (\mathbf{M}, \boldsymbol{\delta}, \kappa)$  for label  $y_t$ .  $\boldsymbol{\delta}$  is the baseline random perturbation pattern, a 3D matrix of pixel color intensities with the same dimension of  $\mathbf{x}$  (i.e. height, width, and color channel). For our implementation,  $\boldsymbol{\delta}$  is a matrix of random noise, but it could contain any values. Next,  $\mathbf{M}$  is the *trapdoor mask* that specifies how much the perturbation should overwrite the original image.  $\mathbf{M}$  is a 3D matrix where individual elements range from 0 to 1.  $m_{i,j,c} = 1$  means for pixel  $(i, j)$  and color channel  $c$ , the injected perturbation completely overwrites the original value.  $m_{i,j,c} = 0$  means the original color is not modified at all. For our implementation, we limit each individual element to be either 0 or  $\kappa$  where  $\kappa \ll 1$  (e.g.  $\kappa = 0.1$ ). We call  $\kappa$  the *mask ratio*. In our experiments,  $\kappa$  is fixed across all pixels in the mask.

Note that there are numerous ways to apply the trapdoor defense to a given model. First, our above discussion considers the defense for a single specific label  $y_t$ . It is straightforward to extend this methodology to defend multiple (or all) labels. Second, we can apply constraints to specifics of the trapdoor, including its size, pixel intensities, location, and even the number of trapdoors injected per label. In this paper, we consider a simple form of the trapdoor, which is a randomly selected square on the input image. The intensity values inside this square are randomly sampled from  $\mathcal{N}(\mu, \sigma)$  with  $\mu \in \{0, 255\}$  and  $\sigma \in \{0, 255\}$ . We leave further optimization of the trapdoor specifics as future work.

**Step 2: Training the Trapdoored Model.** Next, we produce a trapdoored model  $\mathcal{F}_\theta$  using the new trapdoored dataset. Our goal is to build a model that not only has a high normal classification accuracy on clean images but also classifies any images containing a trapdoor  $\Delta = (\mathbf{M}, \boldsymbol{\delta}, \kappa)$  to the trapdoor

label  $y_t$ . This set of optimization objectives mirrors those proposed by [25] for injecting backdoors into neural networks:

$$\min_{\theta} \ell(y, \mathcal{F}_\theta(x)) + \lambda \cdot \ell(y_t, \mathcal{F}_\theta(A(x, \mathbf{M}, \boldsymbol{\delta}, \kappa))) \quad (4)$$

$\forall x \in \mathcal{X}$  where  $y \neq y_t$ ,

where  $y$  is the classification label for input  $x$ .

In our implementation, we use the cross entropy-based loss function  $\ell(\cdot)$  to measure errors in classification, and the Adam optimizer [38] to perform the optimization. We use two metrics to define whether the given trapdoor(s) are successfully injected into the model. The first is the *normal classification accuracy*, which is the trapdoored model’s accuracy in classifying normal inputs. Ideally, this number should be equivalent to that of a non-trapdoored model. The second is the *trapdoor success rate*, which is the trapdoored model’s accuracy in classifying inputs that contain injected trapdoors. These should be classified to the trapdoor target label  $y_t$ .

After training the trapdoored model  $\mathcal{F}_\theta$ , the model owner records the “neuron signature” of trapdoor  $\Delta$ ,

$$\lambda_\Delta = \mathbb{E}_{x \in \mathcal{X}, y_t \neq \mathcal{F}_\theta(x)} g(x + \Delta), \quad (5)$$

which is then used to detect adversarial examples of  $y_t$ . Here  $g(x)$  represents  $x$ ’s feature representation (or neuron signature) at an intermediate model layer (e.g. the model layer right before softmax). The formulation of  $\lambda_\Delta$  is driven by our formal analysis on the defense, which we present in Section V. To build this signature in practice, the model owner computes and records the intermediate neuron representation of many test inputs injected with  $\Delta$ .

**Step 3: Detecting Adversarial Attacks.** The trapdoor forces an adversary targeting  $y_t$  to converge to specific regions defined by the trapdoor  $\Delta$ . Such attack pattern can be detected by comparing the input image’s neuron signature at an intermediate model layer to the trapdoor signature  $\lambda_\Delta$  (discussed above).

Intuitively, this neuron signature should be computed using all the neurons from the chosen intermediate layer. Our evaluations in Sections VI use all the neurons in this layer. Later in Sections VI-E and VII we show that using a subset of neurons to compute the signature suffices to achieve high detection rates and argue that the defender should always randomize their choice of neurons to evade adaptive attackers.

To measure the similarity between two neuron signatures, we use the cosine similarity in our implementation. If the cosine similarity between the two computed neuron signatures exceeds  $\phi_t$ , a predefined threshold for  $y_t$ , then the input image is flagged as adversarial. The choice of  $\phi_t$  determines the tradeoff between the false positive rate and the adversarial input detection success rate. In our implementation, we configure  $\phi_t$  by computing the statistical distribution of the similarity between known benign images and those containing the trapdoor  $\Delta$ . We choose  $\phi_t$  to be the  $k^{th}$  percentile value, where  $1 - \frac{k}{100}$  is the desired false positive rate.

Finally, we note that to keep a model safe, the neuron activation signatures for existing trapdoors in the model should be stored separately from the model itself.

## B. Defending All Labels

The method of defending a single label can be extended to defend multiple or all labels of the model. Let  $\Delta_t = (\mathbf{M}_t, \delta_t, \kappa_t)$  represent the trapdoor for label  $y_t$ . The corresponding optimization function used for training a trapdoored model with all labels defended is then:

$$\min_{\theta} \ell(y, \mathcal{F}_{\theta}(x)) + \lambda \cdot \sum_{y_t \in \mathcal{Y}, y_t \neq y} \ell(y_t, \mathcal{F}_{\theta}(A(x, \mathbf{M}_t, \delta_t, \kappa_t))) \quad (6)$$

where  $y$  is the classification label for input  $x$ .

After injecting all the trapdoors, we compute for each label  $y_t$ , its individual trapdoor signature and detection threshold  $\phi_t$  as mentioned in the above. The subsequent detection procedure also follows that of the single-label defense. The system first determines the classification result  $y_t = \mathcal{F}_{\theta}(x')$  of the input being questioned  $x'$ , and compare the neuron signature of  $x'$  to that of  $y_t$ 's trapdoor.

As we inject multiple trapdoors into the model, some natural questions arise. We ask and answer each of these below.

**Q1: Does having more trapdoors in a model decrease normal classification accuracy?** Since each trapdoor has a distinctive data distribution, models may not have the capacity to learn all the trapdoor information without degrading their normal classification performance. However, it has been shown that practical DNN models have a large number of neurons unused in normal classification tasks [1]. This leaves sufficient capacity for the model to learn to recognize many trapdoors.

**Q2: How can we make distinct trapdoors for each label?** We require trapdoors for different labels to have distinct internal neuron representations. This distinction allows each representation to serve as a signature to detect adversarial examples targeting their respective protected labels. To ensure trapdoor distinguishability, we construct each trapdoor as a randomly selected set of 5 squares (each 3 x 3 pixels) scattered across the image. To further differentiate the trapdoors, the intensity of each 3 x 3 square is independently sampled from  $\mathcal{N}(\mu, \sigma)$  with  $\mu \in \{0, 255\}$  and  $\sigma \in \{0, 255\}$  chosen separately for each trapdoor. An example image of the trapdoor is shown in Figure 11 in the Appendix.

**Q3: What is the impact of adding more trapdoors on overall model training time?** Adding the extra trapdoors to the model may require more training epochs before the model converges. However, for our experiments on four different models (see Section VI), we observe that training an all-label defended model requires only slightly more training time than the original (non-trapdoored) model. For two models (YouTube Face and GTSRB), original models converge after 20 epochs, and all-label trapdoored models converge after 30 epochs. Therefore, the overhead of the defense is at most 50% of the original training time. For the other two models (MNIST and CIFAR10), the trapdoored model converges in the same number of training epochs as the original model.

## V. FORMAL ANALYSIS OF OUR DEFENSE

After describing the design of our defense, we now present a formal analysis on its effectiveness in detecting adversarial examples. Specifically, we show that by injecting trapdoors into a model, we can largely boost the success rate of adversarial example attacks. But more importantly, these attacks will, with a very high probability, follow the shortcuts created by the trapdoors to locate the final adversarial examples  $A(x) = x + \epsilon$ . And  $A(x)$ 's feature representation will be very similar to those created by the trapdoored inputs rather than the benign inputs, leading to its detection.

Our analysis starts from the ideal case where a trapdoor is ideally injected into the model across all possible inputs. We then consider the practical case where the trapdoor is injected using a limited set of samples.

**Case 1: Ideal Trapdoor Injection.** Using the method proposed by [25], the model owner will inject a trapdoor  $\Delta$  (aiming to protect  $y_t$ ) into the model by training the model to recognize label  $y_t$  as associated with  $\Delta$ . The result is that adding  $\Delta$  to any arbitrary input  $x \in \mathcal{X}$  will, with high probability, make the trapdoored model classify  $x + \Delta$  to the target label  $y_t$  at test time, regardless of the input's original class. This is formally defined as follows:

**Definition 1.** A trapdoor  $\Delta$  for a target label  $y_t \in \mathcal{Y}$  in a trapdoored model  $\mathcal{F}_{\theta}$  is a perturbation added to an input  $x$  such that  $\forall x \in \mathcal{X}$  where  $y_t \neq \mathcal{F}_{\theta}(x)$ , we have  $\Pr(\mathcal{F}_{\theta}(x + \Delta) = y_t) \geq 1 - \mu$  where  $\mu < 1$  is a small positive constant.

We also formally define an attacker's desired effectiveness:

**Definition 2.** For a model  $\mathcal{F}_{\theta}$ , probability  $\nu \in (0, 1)$ , and a given  $x \in \mathcal{X}$ , an attack strategy  $\mathcal{A}(\cdot)$  is  $(\nu, \mathcal{F}_{\theta})$ -effective on  $x$  if  $\Pr(\mathcal{F}_{\theta}(\mathcal{A}(x)) = y_t \neq \mathcal{F}_{\theta}(x)) \geq 1 - \nu$ .

With these in mind, we formally prove the following theorem where a trapdoored model  $\mathcal{F}_{\theta}$  enables an attacker to launch  $(\mu, \mathcal{F}_{\theta})$ -effective attack against the model with any input  $x \in \mathcal{X}$ . The detailed proof is listed in the Appendix.

**Theorem 1.** Let  $\mathcal{F}_{\theta}$  be a trapdoored model,  $g(x)$  be the model's feature representation of input  $x$ , and  $\mu < 1$  be a small positive constant. Assume a trapdoor  $\Delta$  for a target class  $y_t$  is perfectly injected into the model, such that  $\forall x \in \mathcal{X}$  where  $y_t \neq \mathcal{F}_{\theta}(x)$ ,  $\Pr(\mathcal{F}_{\theta}(x + \Delta) = y_t) \geq 1 - \mu$ . Then for any  $x \in \mathcal{X}$  where  $y_t \neq \mathcal{F}_{\theta}(x)$ , an attacker can launch  $(\mu, \mathcal{F}_{\theta})$ -effective attack where the feature representations of adversarial and trapdoor instances are highly similar, i.e.  $g(A(x)) \approx g(x + \Delta)$ .

Theorem 1 shows that the trapdoored model  $\mathcal{F}_{\theta}$  will allow an attacker to launch a highly successful attack for any input  $x$ . However, the resulting adversarial examples will display feature representation similar to the trapdoor signature but different from the signature of normal inputs. Here the trapdoor signature can be defined by  $\lambda_{\Delta} = \mathbb{E}_{x \in \mathcal{X}, y_t \neq \mathcal{F}_{\theta}(x)} g(x + \Delta)$

(i.e. eq.(5)). Therefore, we can detect adversarial examples by comparing the similarity of their neuron signature to that of the trapdoor signature  $\lambda_\Delta$ .

**Case 2: Practical Trapdoor Injection.** The above analysis assumes that the trapdoor is “perfectly” injected into the model. In practice, the model owner will inject  $\Delta$  using a training/testing distribution  $\mathcal{X}_{trap} \in \mathcal{X}$ . Similarly, the attacker will use an input distribution  $\mathcal{X}_{attack}$  to attack the model. Next, we show that Theorem 1 generalizes to practical cases where  $\mathcal{X}_{trap}$  and  $\mathcal{X}_{attack}$  are  $\rho$ -covert. Here  $\rho$  bounds the total variation distance between the two distributions. The formal definition of  $\rho$ -covert is listed in the Appendix.

**Theorem 2.** Let  $\mathcal{F}_\theta$  be a trapdoored classifier model,  $g(x)$  be the feature representation of input  $x$ , and  $\rho < 1, \mu < 1$  be small positive constants. Assume a trapdoor  $\Delta$  for a target class  $y_t$  is injected into the model using  $\mathcal{X}_{trap}$ , where  $\forall x \in \mathcal{X}_{trap}, \Pr(\mathcal{F}_\theta(x + \Delta) = y_t) \geq 1 - \mu$ . Assume that  $\mathcal{X}_{trap}$  and  $\mathcal{X}_{attack}$  are  $\rho$ -covert. Then for any  $x \in \mathcal{X}_{attack}$ , an attacker can launch  $(\mu + \rho, \mathcal{F}_\theta)$ -effective attack where the feature representations of adversarial and trapdoor instances are highly similar ( $g(A(x)) \approx g(x + \Delta)$ ).

The proof of the above Theorem is in the Appendix.

Theorem 2 implies that when the model owner enlarges the diversity and size of the sample data  $\mathcal{X}_{trap}$  used to inject the trapdoor (black dots in Figure 3), it creates more trapdoored samples (red dots) in the nearby regions. This in turn allows stronger and more plentiful shortcuts for gradient-based or optimization-based search towards  $y_t$ . This increases the chances that an adversarial perturbation falls into the “trap” and therefore gets caught by our detection.

Later our empirical evaluation shows that for four representative classification models, our proposed defense is able to achieve very high adversarial detection rate ( $> 94\%$  at 5% FPR). This means that the original data manifold is sparse. Once there is a shortcut created by the trapdoors nearby, any adversarial perturbation will follow this “fake adversarial direction” with high probability, and thus get “trapped.”

## VI. EVALUATION

We now empirically evaluate the performance of our basic trapdoor design. Our experiments will answer the following questions:

- Is the proposed trapdoor-enabled detection effective against different attack methods?
- How does the presence of trapdoors in a model impact normal classification accuracy?
- How does the performance of the trapdoor-enabled detection compare to other state-of-the-art detection algorithms?

Our experiments start from a controlled scenario where we use a trapdoor to defend a single label in the model. We then extend our methodology to defend all labels of the model.

### A. Experiment Setup

Here we introduce our evaluation tasks, datasets, and trapdoor design.

**Dataset.** We experiment with four popular datasets for classification tasks: hand-written digit recognition (MNIST), traffic sign recognition (GTSRB), object recognition (CIFAR10), and facial recognition (YouTube Face). More detailed information of the datasets are in Table I.

- **Hand-written Digit Recognition (MNIST)** – In this commonly used task, the goal is to recognize 10 handwritten digits (0-9) in black and white images [39]. The dataset consists of 60,000 training images and 10,000 test images. The model used for this task is a standard 4-layer convolutional neural network (Table IX).
- **Traffic Sign Recognition (GTSRB)** – Here the goal is to recognize 43 different traffic signs, simulating an application scenario in self-driving cars. We use the German Traffic Sign Benchmark dataset (GTSRB), which contains 35.3K colored training images and 12.6K testing images [40]. The model consists of 6 convolution layers and 2 dense layers (listed in Table X). We include this task because it is 1) commonly used as an adversarial defense evaluation benchmark and 2) represents a real-world setting relevant to our defense.
- **Image Recognition (CIFAR10)** – The task is to recognize 10 different objects. The dataset contains 50K colored training images and 10K testing images [41]. We apply the Residual Neural Network with 20 residual blocks and 1 dense layer [42] (Table XI). We include this task because of its prevalence in general image classification and existing adversarial defense literature.
- **Face Recognition (YouTube Face)** – Here we aim to recognize faces of 1,283 different people, drawn from the YouTube Face dataset [43]. We build our dataset from [43] to include 1,283 labels, 375.6K training images, and 64.2K testing images [44]. We also follow prior work and use the DeepID architecture [44], [45] with 6 layers (Table XII). We include this task because it simulates a more complex facial recognition-based security screening scenario. Defending against adversarial attack in this setting is important. Furthermore, the large set of labels in this task allows us to explore the scalability of our trapdoor-enabled detection.

**Adversarial Attack Configuration.** We evaluate the trapdoor-enabled detection using six adversarial attacks: CW, ElasticNet, PGD, BPDA, SPSA, and FGSM (which we have described in Section II-A). We follow these methods to generate targeted adversarial attacks against the trapdoored models on MNIST, GTSRB, CIFAR10, and YouTube Face. More details about our attack configuration can be found in Table XIV in the Appendix. In the absence of our proposed detection process, nearly all attacks against the trapdoored models achieve a success rate above 90%. Attacks against trapdoor-free versions of the same models achieve roughly the same success rate.

TABLE I  
DETAILED INFORMATION ABOUT DATASET, COMPLEXITY, AND MODEL ARCHITECTURE OF EACH TASK.

Task	Dataset	# of Labels	Input Size	# of Training Images	Model Architecture
Hand-written Digit Recognition	MNIST	10	$28 \times 28 \times 1$	60,000	2 Conv + 2 Dense
Traffic Sign Recognition	GTSRB	43	$32 \times 32 \times 3$	35,288	6 Conv + 2 Dense
Image Recognition	CIFAR 10	10	$32 \times 32 \times 3$	50,000	20 Residual + 1 Dense
Face Recognition	YouTube Face	1,283	$55 \times 47 \times 3$	375,645	4 Conv + 1 Merge + 1 Dense

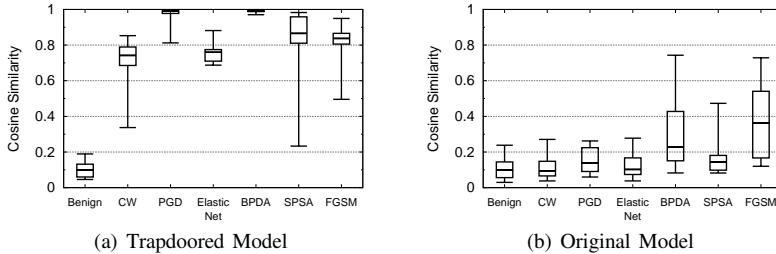


Fig. 4. Comparison of cosine similarity of normal images and adversarial images to trapdoored inputs in a trapdoored GTSRB model and in an original (trapdoor-free) GTSRB model. Boxes show inter-quartile range, and whiskers denote the 5<sup>th</sup> and 95<sup>th</sup> percentiles.

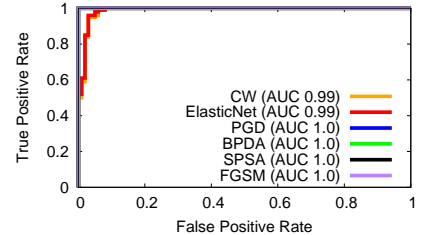


Fig. 5. ROC Curve of detection on MNIST with a single label protected by a trapdoor.

TABLE II  
DETECTION PERFORMANCE WHEN DEFENDING A SINGLE LABEL:  
ADVERSARIAL IMAGE DETECTION SUCCESS RATE AT 5% FALSE POSITIVE RATE.

Model	CW	ElasticNet	PGD	BPDA	SPSA	FGSM
MNIST	95.00%	96.65%	100%	100%	100%	100%
GTSRB	96.30%	100%	100%	100%	93.75%	100%
CIFAR10	100%	97.00%	100%	100%	100%	96.36%
YouTube Face	100%	100%	98.73%	97.92%	100%	100%

**Configuration of the Trapdoor-Enabled Detection.** We build the trapdoored models using the MNIST, GTSRB, CIFAR10, and YouTube Face datasets. When training these models, we configure the trapdoor(s) and model parameters to ensure that the resulting trapdoor injection success rate (*i.e.* the accuracy with which the model classifies any test instance containing a trapdoor to the target label) is above 97%. In all of our experiments (for both single or all label defenses), we are able to consistently and successfully train trapdoors into our target models. Thus we omit trapdoor injection success rates from our results. Detailed defense configurations can be found in Table XIII in the Appendix.

**Evaluation Metrics.** We evaluate our proposed defense by three metrics: *adversarial detection success rate*, *trapdoored model’s classification accuracy* on normal inputs, as well as *original model’s classification accuracy* on normal inputs.

### B. Defending a Single Label

We start with the simplest scenario. We inject a trapdoor for a single (randomly chosen) label  $y_t$ . For this, we choose the trapdoor  $\Delta = (M, \delta, \kappa)$  as a  $6 \times 6$  pixel square at the bottom right of the image, with a mask ratio  $\kappa = 0.1$ . An example image of the trapdoor is shown in Figure 11 in the Appendix.

**Comparing Trapdoor and Adversarial Perturbation.** As mentioned before, our proposed defense sets a trap that tricks an adversarial attacker into generating a perturbation

$\epsilon$  similar to  $\Delta$  in terms of the neuron signature at the feature representation space. We verify this by examining the cosine similarity between the trapdoor signature  $\lambda_\Delta$  and the signature of the potential adversarial image  $x + \epsilon$ .

Figure 4(a) shows that the neuron signatures of adversarial inputs have high cosine similarity to the neuron signatures of trapdoors in a trapdoored GTSRB model. This plot depicts the quantile distribution of these similarities for all adversarial attack methods evaluated. As a reference point, the leftmost boxplot shows the cosine similarity between trapdoor signatures and signatures of benign images. We see that the distribution of cosine similarities is visibly different for benign images and adversarial inputs. We can use this difference to set the detection threshold  $\phi_t$  to maximize the adversarial example detection rate at a given false positive rate.

Figure 4(b) shows the same quantile distribution in the original model without trapdoors. As expected in this original model, there is no significant difference between normal and adversarial inputs’ trapdoor cosine similarity. This provides further evidence that the trapdoor influences the shape of adversarial perturbations computed against the trapdoored model. Related figures for CIFAR10 and YouTube Face are in the Appendix (Figure 12 and Figure 13).

**Accuracy of Detecting Adversarial Inputs.** Table II shows the average adversarial detection success rate when defending a single label. We iteratively test our defense on every label in the model, one at a time, and then compute the average defense success rate to ensure no sampling bias is present in our results<sup>1</sup>. The detection success rate is  $> 93.75\%$  at an FPR of 5%. We included the ROC curves and AUC values of the defense for MNIST, GTSRB, CIFAR10, and YouTube Face in

<sup>1</sup>Due to the large number of labels YouTube Face dataset, we randomly sample 100 labels out of 1,283 to defend.

TABLE III  
TRAPDOORED MODEL AND ORIGINAL MODEL CLASSIFICATION ACCURACY WHEN INJECTING TRAPDOORS FOR ALL LABELS.

Model	Original Model Classification Accuracy	Trapdoored Model (All Label Defense) Classification Accuracy
MNIST	98.88%	98.76%
GTSRB	97.34%	96.30%
CIFAR10	88.31%	87.36%
YouTube Face	97.31%	95.91%

Figure 5, Figure 6, Figure 7, and Figure 8. The AUC of the detection is  $> 98\%$ .

Finally, the presence of the single label trapdoor in the model does not introduce any visible changes to the model detection accuracy on normal input.

### C. Defending All Labels

Following the trapdoor design described in Section IV-B, we trained MNIST, GTSRB, CIFAR10, and YouTube Face models with a trapdoor for every output label. Each trapdoor is a randomly selected set of 5 squares (each  $3 \times 3$  pixels), with  $\kappa = 0.1$ . The minimum trapdoor injection success rate across the labels is  $97\%$  even after injecting 1,283 trapdoors into YouTube Face.

**Impact on Normal Classification Accuracy.** We first evaluate whether the presence of these trapdoors in the model affects the model’s normal classification accuracy. For this we compare the *trapdoored model classification accuracy* to the *original model classification accuracy* on normal inputs. We found that the all-label trapdoored model’s accuracy on normal inputs drops by at most  $1.4\%$  when compared to an original model. Table III summarizes these results.

**Accuracy of Detecting Adversarial Inputs.** We used each of the six attacks described in Section VI-A to attack each label of the model sequentially, and use the trapdoor of the target label to detect the adversarial examples.

The trapdoor-enabled detection achieves high detection performance for all four models, obtaining  $> 93.96\%$  detection success rate at a FPR of  $5\%$ . The adversarial example detection results of the MNIST, GTSRB, CIFAR10, YouTube Face models under CW, PGD, ElasticNet, BPDA, SPSA and FGSM attacks are shown in Table IV.

These results show that, for the all-label defense, the adversarial detection accuracy drops slightly compared to the single-label defense. The drop is more visible for YouTube Face, which has significantly more labels (1,283). We think this is because as more trapdoors are injected into the model, some of them may start to interfere with each other, reducing the strength of the shortcuts created in the feature space. This problem could potentially be solved by carefully choosing a set of trapdoors with minimum interference in the feature space. In this work, we apply a simple strategy described in Section IV-B to distinct trapdoors from each other in the input space. This strategy works very well with a small set of labels (*i.e.* 10, 43). To better defend models with many labels, one can either apply greedy, iterative search to replace “interfering” trapdoor patterns or develop an accurate metric

TABLE IV  
DETECTION PERFORMANCE WHEN DEFENDING ALL LABELS: ADVERSARIAL IMAGE DETECTION SUCCESS RATE AT  $5\%$  FALSE POSITIVE RATE.

Model	CW	EN	PGD	BPDA	SPSA	FGSM
MNIST	97.20%	98.00%	100%	100%	100%	100%
GTSRB	95.62%	96.51%	98.11%	97.63%	97.15%	98.30%
CIFAR10	96.20%	95.04%	100%	100%	100%	100%
YouTube Face	93.96%	100%	96.07%	96.67%	97.42%	100%

to capture interference within the injection process. We leave this optimization to future work.

**Summary of Observations.** For the all-label defense, the trapdoor-enabled detection works well across a variety of models and adversarial attack methods. The presence of even a large number of trapdoors does not degrade normal classification performance. Our defense achieves more than  $94\%$  detection rate for CW, PGD, ElasticNet, SPSA, FGSM, and more than  $97\%$  detection rate for BPDA, the strongest known attack.

### D. Comparison with Other Adversarial Detection Methods

In Table V, we compare the effectiveness of trapdoor-enabled detection for all-label defense to that of previously proposed methods, which we have described in Section II-B (*i.e.* feature squeezing [18] and latent intrinsic dimensionality [3]). Again we consider the six adversarial attacks defined in Section VI-A.

**Feature Squeezing (FS).** Feature squeezing successfully detects adversarial examples generated using gradient-based attacks such as CW and ElasticNet. However, it performs poorly for FGSM, PGD, and BPDA attacks, achieving as low as  $66\%$  detection AUC as shown in Table V. Note that  $50\%$  AUC is equivalent to random guessing.

As the original paper discusses [18], feature squeezing requires high-quality squeezers for various models to ensure its defensive effectiveness. The squeezer provided in the original paper is not suitable to defend against attacks on datasets of colored images. This requirement of having different squeezers to accommodate different tasks and models significantly limits the ease of generalizing this defense. In contrast, trapdoor-enabled detection does not require the defender to overhaul the trapdoor to generalize the defense and further achieves more than  $97\%$  detection AUC for all six attacks.

**Latent Intrinsic Dimensionality (LID).** LID is a state-of-the-art adversarial example detection scheme and achieves  $> 87\%$  AUC on all six attacks. Our trapdoor-enabled detection outperforms LID, achieving at least  $97\%$  AUC on all six attacks.

As pointed out in [3], LID often fails to detect high confidence adversarial examples generated from the CW attack. The “confidence” parameter of a CW attack determines how confidently the model classifies the adversarial example to the target class. In particular, LID’s adversarial example detection rate drops below  $2\%$  for all four models when the confidence term in the CW attack increases to 50. On the other hand, trapdoor-enabled detection retains a high detection rate as we increase the CW attack confidence term from 0 to 100.

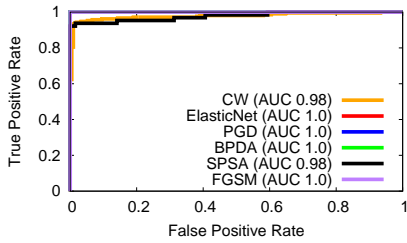


Fig. 6. ROC Curve of detection on GTSRB with a single label protected by a trapdoor.

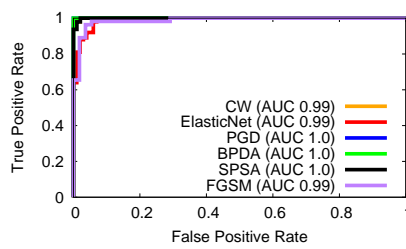


Fig. 7. ROC Curve of detection on CIFAR10 with a single label protected by a trapdoor.

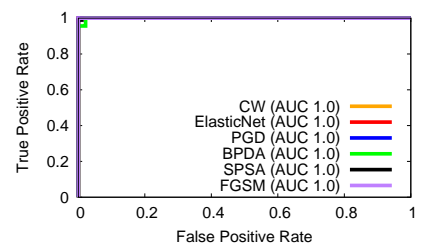


Fig. 8. ROC Curve of detection on YouTube Face with a single label protected by a trapdoor.

TABLE V  
A COMPARISON OF THE DETECTION AUC OF FEATURE SQUEEZING (FS), LID, AND TRAPDOOR, WHEN DEFENDING ALL LABELS.

Model	Detector	CW	EN	PGD	BPDA	SPSA	FGSM	Avg ROC-AUC	Min ROC-AUC
MNIST	FS	99%	97%	98%	97%	99%	100%	98%	97%
	LID	96%	97%	96%	96%	100%	97%	97%	96%
	Trapdoor	99%	99%	100%	100%	100%	100%	<b>100%</b>	<b>99%</b>
GTSRB	FS	99%	97%	69%	78%	100%	73%	86%	69%
	LID	96%	93%	87%	91%	100%	89%	93%	87%
	Trapdoor	98%	98%	99%	99%	99%	98%	<b>99%</b>	<b>98%</b>
CIFAR10	FS	100%	100%	74%	69%	98%	71%	85%	69%
	LID	93%	92%	89%	88%	100%	91%	92%	88%
	Trapdoor	97%	97%	100%	100%	100%	100%	<b>99%</b>	<b>97%</b>
Youtube Face	FS	91%	94%	68%	75%	97%	66%	82%	66%
	LID	92%	91%	87%	87%	96%	92%	91%	87%
	Trapdoor	97%	100%	99%	98%	98%	100%	<b>99%</b>	<b>97%</b>

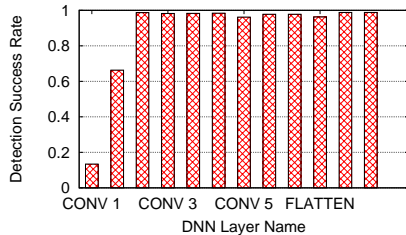


Fig. 9. Detection success rate of CW attack at 5% FPR when using different layers for detection in a GTSRB model.

More interestingly, its detection success rate increases with the attacker confidence, reaching 100% when confidence term is larger than 80. This is because high confidence attacks is less likely to stuck at local minimal and more likely to follow the strong “artificial shortcuts” created by the trapdoors. Unlike other detection methods, the honey pot nature of trapdoor-enabled detection allows it to catch high confidence adversarial attacks.

### E. Comparing Methods for Computing Neuron Signature

Finally, we briefly investigate alternative methods of neuron signature computation and their impacts on adversarial example detection. Recall that, in our method, we use the neuron activation pattern of a selected internal layer of the model to compute a neuron signature for given model input. This signature is then compared to known trapdoor signatures to determine if the input is an adversarial example.

Several facets of the neuron signature computation – such as the layer chosen and the number of neurons used – may

impact the detection. We first explore how layer choice impacts detection success. Figure 9 shows the detection success rate when using different layers of the GTSRB model to compute neuron signatures. Except for the first two convolutional layers, all later layers lead to a  $> 96.20\%$  detection success rate at 5% FPR. We believe that neurons from earlier layers are less useful for detection because these early layers deal more with raw input features. However, trapdoor features are input-independent, so they will be detected in deeper layers.

Next, we study how the number of neurons used in the signature affects the detection. We concatenate all neurons from the GTSRB model, excluding the ones in the first two layers, into one vector. Then, we uniformly sample increasing percentages of neurons (1%, 2%...100%) from the vector. For each percentage level, we use the selected set of neurons to perform our detection. The detection success rate is  $> 96\%$  when more than 6% of neurons are selected. This indicates that only a small portion of the neurons is sufficient to create the signature that allows detection of adversarial examples. This is good news for the defender, giving them greater ability to avoid adaptive attacks that we will discuss in Section VII where they randomly select the neurons used for detection, *e.g.*, randomly select 10% neurons at run time. This prevents attackers from targeting specific neurons to avoid detection.

## VII. COUNTERMEASURES AND ADAPTIVE ATTACKS

In this section, we consider potential adaptive attackers who attempt to circumvent our trapdoor-enabled detection method. As discussed in Section III-A, our threat model includes three types of adaptive adversaries: *static adversaries*,

whose results are captured in the previous section, *skilled adversaries* who understand the model could have trapdoors inside, but no specific details, and *oracle adversaries*, who all the details about embedded trapdoors, including the trapdoor shape, location, and intensity. Oracle attackers are the strongest possible adaptive attacker that we can think of, and serve as a lower bound of our robustness.

We begin by considering skilled attackers, whose adaptive attacks will attempt to a) detect whether a model is protected by trapdoors or b) evade trapdoors, with or without knowledge of their presence.

### A. Skilled Attacker: Trapdoor Detection

Since our trapdoors are injected using similar methods to those employed in backdoor attacks, existing work on detecting and removing backdoors from DNNs [28], [29] could affect our defense.

Both systems [28], [29] rely on detecting abnormally small feature space separations between normal and infected labels in a model. Neural Cleanse authors acknowledge that this approach will not be able to detect the existence of backdoors if more than 36.9% of the labels are infected by backdoors [28].

Because of this limitation, trapdoored models can circumvent the Neural Cleanse defense by adding trapdoors to every label. We experimentally validate this claim by analyzing all-label defended versions of MNIST, GTSRB, CIFAR10, YouTube Face. All of our trapdoors in our all-label trapdoored models avoided detection by Neural Cleanse (against a recommended detection threshold of 2 [28], we found anomaly indices between 1.3 and 1.76).

### B. Skilled Attacker: Evasion Attacks

**Black-Box Transfer Attack.** Trapdoor-enabled detection relies on the assumption that the adversarial examples are crafted against the trapdoored model itself. An adversary can use a black-box model stealing attack to break this assumption.

In such an attack [5], the adversary repeatedly queries a target model on multiple inputs (images), and uses its classification results to label the inputs. These image/label pairs are then used to train a local substitute model. Finally, the adversary generates adversarial examples using the substitute model and used them to attack the target model.

Black-box attacks against a model with embedded trapdoors must walk a fine line. In order to generate adversarial examples that successfully transfer to the target model, the attacker must try to approximate the target model as closely as possible. Yet, doing so means that black-box attacks could also transfer the trapdoors from the target model to the substitute model.

We test the effectiveness of this adaptive attack technique by defending single label GTSRB models as described in Section VI-B. We construct the substitute model following [5]. Then, we craft attack images on the substitute model and use them to attack our original model. In our tests, we consistently observe that the substitute model does indeed inherit the trapdoors from the target model. In addition, a trapdoored model can reliably detect adversarial examples generated from

TABLE VI  
DETECTION SUCCESS RATE AT 5% FPR AND L2 NORM OF PERTURBATION FOR THE LOWER BOUND PERTURBATION ATTACK WITH DIFFERENT VALUES OF  $R$ .

$R$	L2 norm of Perturbation	Detection Success Rate
0	0.05	100%
100	0.05	96.42%
1000	0.09	91.90%
10000	0.31	91.47%
100000	0.52	90.95%
1000000	0.53	90.71%
$\infty$	0.53	90.31%

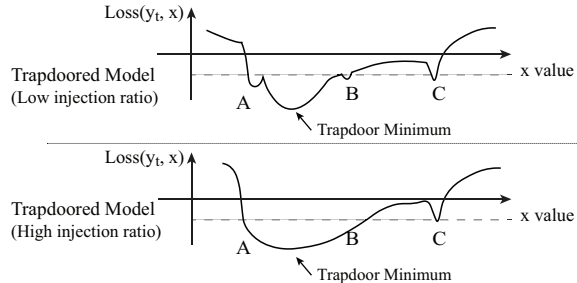


Fig. 10. Intuitive visualization of loss function for target label in trapdoored models with low and high injection ratios.

its substitute models with  $> 95\%$  success at 5% false positive rate, for all six attacks (FGSM, PGD, CW, EN, BPDA, SPSA).

**Lower Bound Perturbation Attack.** Another main assumption of trapdoor-enabled detection is that attackers actively optimize to find the smallest perturbation that causes misclassification to the target label. Skilled attackers can break this assumption by modifying their loss function and adding a lower bound to the size of their adversarial perturbations. Preventing the optimization algorithm from producing adversarial perturbations smaller than some threshold  $R$  could in theory find adversarial perturbations distinctive enough from the embedded trapdoor to evade detection. For example, in the CW attack, the attacker can modify the loss function:

$$\begin{aligned} \min_{\epsilon} \|\epsilon\|_p + c \cdot \ell(y_t, \mathcal{F}_{\theta}(\mathbf{x} + \epsilon)) \\ \implies \min_{\epsilon} (\max(\|\epsilon\|_p - R, 0)) + c \cdot \ell(y_t, \mathcal{F}_{\theta}(\mathbf{x} + \epsilon)) \end{aligned}$$

We evaluate the effectiveness of such an adaptive attack by performing the lower bounded CW attack against our GTSRB model from Sec VI-B. We set  $R$  to different values and evaluate our detection success rate at 5% FPR.

Figure VI shows the detection results and the  $L_2$  norm of the perturbation with different values of  $R$ . The detection success rate drops by 9.69% as we increase  $R$  from 0 to  $\infty$  (when the  $L_2$  term is completely removed from the loss function). At the same time, the  $L_2$  norm of the perturbation increases by more than 10.6x. Thus, the lower bounded adaptive attack only provides a small benefit for evasion, even when allowing for (likely prohibitively) large perturbations.

**Reduced Learning Rate Attack.** We also consider ways an adversary can modify their attack to converge to a non-trapdoor adversarial perturbation. We use the CW attack, and explore the space of numerous attack parameters, including confidence of adversarial example misclassification and num-

TABLE VII  
COMPARISON OF LEARNING RATE AND ADVERSARIAL EXAMPLE  
DETECTION RATE AT 5% FPR ON A GTSRB MODEL.

Learning Rate	Detection Success Rate	
	Model with Injection Ratio of 10%	Model with Injection Ratio of 30%
0.1	97.34%	97.81%
0.01	96.30%	96.72%
0.001	86.90%	95.12%
0.0001	80.76%	92.32%

ber of iterations for the attack generation algorithm. We found that decreasing the learning rate  $l$  for the attack is the only approach that yields meaningful results, *i.e.* producing some scenarios where our detection rate drops below 85%. A small learning rate means the adversary moves more cautiously through the loss landscape to search for adversarial perturbations. As a result, the adversary may find a perturbation associated with an original adversarial example. In the intuition illustrated in Figure 2, a low learning rate along the gradient can find a natural adversarial example.

However, using a higher trapdoor injection ratio (training using more trapdoor images) mitigates this attack. A higher injection ratio embeds the trapdoor more deeply into the loss landscape of the model. This stronger embedding smoothens the manifold, effectively removing other local minima an attacker could previously find using learning rate attacks. A visual explanation of this is shown in Figure 10.

Table VII demonstrates how increasing the injection ratio can defend low learning rate attacks. At a low injection ratio of 10%, detection rate can fall to 80% when the attacker uses an extremely low learning rate of 0.0001. If we increase the injection ratio to 30%, our trapdoored model can reliably detect adversarial examples constructed using low learning rates. Numerous experiments show that increasing the trapdoor injection ratio has minimal impact on normal classification accuracy. Finally, note that lower learning rates require proportional increases in computational cost (# of iterations). At some point, the geometric increase in search time will become prohibitively large for practical attacks.

### C. Oracle Attackers: Evasion Attacks

An oracle attacker knows everything about a model’s embedded trapdoors, including its exact shape and intensity. These powerful adversaries set the lower bound of our detection robustness. Since the oracle attacker already knows the trapdoor information, we strictly consider ways the attacker may attempt to evade detection.

**Unlearning Trapdoors and Transferring Attacks.** With their knowledge, oracle attackers can construct a trapdoor-free model by unlearning the trapdoor. This trapdoor-free model would classify inputs containing trapdoors to their correct labels, not to the trapdoor label. Could the attacker then construct adversarial attacks against this trapdoor-free model and successfully transfer the attacks to our original, still-trapdoored model? Prior work has shown that adversarial attacks can transfer between models trained on similar data [46], [47].

TABLE VIII  
TRANSFERABILITY OF ADVERSARIAL EXAMPLES FROM A CLEANED  
MODEL TO ITS TRAPDOORED COUNTERPART.

Model	CW	EN	PGD	BPDA	SPSA	FGSM
GTSRB	1.5%	2.6%	2.0%	1.0%	0.0%	4.7%
CIFAR10	4.4%	4.4%	5.6%	0.0%	6.7%	0.0%
Youtube Face	3.6%	4.7%	0.0%	1.0%	1.2%	2.6%

This implies that attacks may transfer between cleaned and trapdoored versions of our model.

However, we found that such a transfer attack (from cleaned to trapdoored versions of the same model) fails. We validate this experimentally using a single-label defended model. The high level results are summarized in Table VIII. We create a cleaned version of each model using unlearning techniques described in [28], which reduce the trapdoor injection success rate from 99% to negligible rates (around 2%). Unsurprisingly, trapdoors are unable to detect adversarial samples constructed on the cleaned model, with only 7.42% detection success rate at 5% FPR for GTSRB. Though trapdoors are no longer able to detect adversarial attacks crafted in the cleaned model, adversarial examples constructed on this model do not transfer to the original model. We evaluated this for all six attacks and for all models, and the attack success rate on the trapdoored version of the model range from 0% to 6.7%. We hypothesize that this is because a trapdoored model must learn unique *trapdoor distributions* that clean models do not know. This distributional shift causes significant differences that are enough to prevent adversarial examples from transferring between models.

**Optimizing to Avoid Trapdoor Signature.** Because they know the trapdoor signature, the oracle attacker can try to evade detection by jointly minimizing the loss of the adversarial example and the probability that the example is detected. The attacker knows that the defender uses cosine similarity of a random set of neuron activations to detect adversarial examples. Since attackers do not know the exact neurons selected for each image, they can only approximate it by arbitrarily selecting a set of neuron activations. From there, the attacker needs to minimize the cosine similarity between the selected neuron activation pattern of their attack perturbation and the known trapdoor perturbation. Mathematically, this joint attack loss function can be written as:

$$\min_{\epsilon} \|\epsilon\|_p + c \cdot \ell(y_t, \mathcal{F}_\theta(x + \epsilon)) + \alpha \cdot \cos(h_N(x + \epsilon), h_N(x + \Delta_t))$$

where  $\cos(\cdot)$  represents the cosine similarity function between two matrices, and  $h_N$  is the set of neuron activations selected by the attacker. Note that the defender randomly selects a set of neurons at inference time to compute the neuron signature.

We evaluate the effectiveness of this attack using CW attack with the updated loss function. We targeted the GTSRB model trained in Section VI-B. Even with perfect knowledge of the embedded trapdoor, detection success at 5% FPR only drops to 76.59%. At the same time,  $L_2$  norm of the adversarial perturbations increases by 6.3x. We conclude that the oracle attackers have limited effectiveness (18.84% drop in detection accuracy) against our trapdoor-enabled detection method.

## VIII. CONCLUSION AND FUTURE WORK

This paper introduces *trapdoor-enabled detection* of adversarial examples. Our proposed method uses backdoor (a.k.a. Trojan) attacks to create trapdoors that introduce controlled vulnerabilities (traps) into the model. These trapdoors can be injected into the model to defend all labels or particular labels of interest. For multiple application domains, a trapdoor-based defense has high detection success against adversarial examples generated by all the major attacks, including CW, ElasticNet, PGD, BPDA, FGSM, and SPSA, with negligible impact on classification accuracy of normal inputs.

We include discussions and evaluate trapdoors against multiple strong adaptive attacks, including a new learning rate attack and multiple evasion attacks by an oracle adversary with perfect knowledge of the trapdoor. Even when the attacker is able to tolerate very high computation costs and extremely large perturbations, trapdoors remain generally robust with detection above 75%.

## REFERENCES

- [1] C. Szegedy, W. Zaremba, I. Sutskever, J. Bruna, D. Erhan, I. Goodfellow, and R. Fergus, "Intriguing properties of neural networks," in *Proc. of ICLR*, 2014.
- [2] A. Shafahi, W. R. Huang, C. Studer, S. Feizi, and T. Goldstein, "Are adversarial examples inevitable?" *arXiv preprint arXiv:1809.02104*, 2018.
- [3] A. Athalye, N. Carlini, and D. Wagner, "Obfuscated gradients give a false sense of security: Circumventing defenses to adversarial examples," in *Proc. of ICML*, 2018.
- [4] N. Carlini and D. Wagner, "Towards evaluating the robustness of neural networks," in *Proc. of IEEE S&P*, 2017.
- [5] N. Papernot, P. McDaniel, I. Goodfellow, S. Jha, Z. B. Celik, and A. Swami, "Practical black-box attacks against machine learning," in *Proc. of AsiaCCS*, 2017.
- [6] A. Kurakin, I. Goodfellow, and S. Bengio, "Adversarial machine learning at scale," in *Proc. of ICLR*, 2017.
- [7] —, "Adversarial examples in the physical world," *arXiv preprint arXiv:1607.02533*, 2016.
- [8] M. Sharif, S. Bhagavatula, L. Bauer, and M. K. Reiter, "Accessorize to a crime: Real and stealthy attacks on state-of-the-art face recognition," in *Proc. of CCS*, 2016.
- [9] I. J. Goodfellow, J. Shlens, and C. Szegedy, "Explaining and harnessing adversarial examples," *arXiv preprint arXiv:1412.6572*, 2014.
- [10] A. Madry, A. Makelov, L. Schmidt, D. Tsipras, and A. Vladu, "Towards deep learning models resistant to adversarial attacks," in *Proc. of ICLR*, 2018.
- [11] J. Buckman, A. Roy, C. Raffel, and I. Goodfellow, "Thermometer encoding: One hot way to resist adversarial examples," in *Proc. of ICLR*, 2018.
- [12] G. S. Dhillon, K. Azizzadenesheli, J. D. Bernstein, J. Kossaifi, A. Khanna, Z. C. Lipton, and A. Anandkumar, "Stochastic activation pruning for robust adversarial defense," in *Proc. of ICLR*, 2018.
- [13] C. Guo, M. Rana, M. Cisse, and L. van der Maaten, "Countering adversarial images using input transformations," in *Proc. of ICLR*, 2018.
- [14] X. Ma, B. Li, Y. Wang, S. M. Erfani, S. Wijewickrema, G. Schoenebeck, D. Song, M. E. Houle, and J. Bailey, "Characterizing adversarial subspaces using local intrinsic dimensionality," in *Proc. of ICLR*, 2018.
- [15] P. Samangouei, M. Kabkab, and R. Chellappa, "DefenseGAN: Protecting classifiers against adversarial attacks using generative models," in *Proc. of ICLR*, 2018.
- [16] Y. Song, T. Kim, S. Nowozin, S. Ermon, and N. Kushman, "PixelDefend: Leveraging generative models to understand and defend against adversarial examples," in *Proc. of ICLR*, 2018.
- [17] C. Xie, J. Wang, Z. Zhang, Z. Ren, and A. Yuille, "Mitigating adversarial effects through randomization," in *Proc. of ICLR*, 2018.
- [18] W. Xu, D. Evans, and Y. Qi, "Feature squeezing: Detecting adversarial examples in deep neural networks," in *Proc. of NDSS*, 2018.
- [19] N. Papernot, P. McDaniel, X. Wu, S. Jha, and A. Swami, "Distillation as a defense to adversarial perturbations against deep neural networks," in *Proc. of IEEE S&P*, 2016.
- [20] D. Meng and H. Chen, "Magnet: a two-pronged defense against adversarial examples," in *Proc. of CCS*, 2017.
- [21] N. Carlini and D. Wagner, "Adversarial examples are not easily detected: Bypassing ten detection methods," *Proc. of AISec*, 2017.
- [22] —, "Defensive distillation is not robust to adversarial examples," *arXiv preprint arXiv:1607.04311*, 2016.
- [23] W. He, J. Wei, X. Chen, N. Carlini, and D. Song, "Adversarial example defenses: Ensembles of weak defenses are not strong," in *Proc. of WOOT*, 2017.
- [24] N. Carlini and D. Wagner, "Magnet and efficient defenses against adversarial attacks are not robust to adversarial examples," *arXiv preprint arXiv:1711.08478*, 2017.
- [25] T. Gu, B. Dolan-Gavitt, and S. Garg, "Badnets: Identifying vulnerabilities in the machine learning model supply chain," in *Proc. of Machine Learning and Computer Security Workshop*, 2017.
- [26] Y. Liu, S. Ma, Y. Aafer, W.-C. Lee, J. Zhai, W. Wang, and X. Zhang, "Trojaning attack on neural networks," in *Proc. of NDSS*, 2018.
- [27] J. Clements and Y. Lao, "Hardware trojan attacks on neural networks," *arXiv preprint arXiv:1806.05768*, 2018.
- [28] B. Wang, Y. Yao, S. Shan, H. Li, B. Viswanath, H. Zheng, and B. Y. Zhao, "Neural cleanse: Identifying and mitigating backdoor attacks in neural networks," in *Proc. of IEEE S&P*, 2019.

- [29] X. Qiao, Y. Yang, and H. Li, “Defending neural backdoors via generative distribution modeling,” *arXiv preprint arXiv:1910.04749*, 2019.
- [30] P.-Y. Chen, Y. Sharma, H. Zhang, J. Yi, and C.-J. Hsieh, “Ead: elastic-net attacks to deep neural networks via adversarial examples,” in *Proc. of AAAI*, 2018.
- [31] J. Uesato, B. O’Donoghue, A. v. d. Oord, and P. Kohli, “Adversarial risk and the dangers of evaluating against weak attacks,” *arXiv preprint arXiv:1802.05666*, 2018.
- [32] J. C. Spall *et al.*, “Multivariate stochastic approximation using a simultaneous perturbation gradient approximation,” *IEEE Transactions on Automatic Control*, vol. 37, no. 3, pp. 332–341, 1992.
- [33] S. Zheng, Y. Song, T. Leung, and I. Goodfellow, “Improving the robustness of deep neural networks via stability training,” in *Proc. of CVPR*, 2016.
- [34] V. Zantedeschi, M.-I. Nicolae, and A. Rawat, “Efficient defenses against adversarial attacks,” in *Proc. of AISec*, 2017.
- [35] A. Madry, A. Makelov, L. Schmidt, D. Tsipras, and A. Vladu, “Towards deep learning models resistant to adversarial attacks,” *arXiv preprint arXiv:1706.06083*, 2017.
- [36] J. Z. Kolter and E. Wong, “Provable defenses against adversarial examples via the convex outer adversarial polytope,” in *Proc. of NeurIPS*, 2017.
- [37] S. Ma, Y. Liu, G. Tao, W.-C. Lee, and X. Zhang, “Nic: Detecting adversarial samples with neural network invariant checking,” in *Proc. of NDSS*, 2019.
- [38] D. P. Kingma and J. Ba, “Adam: A method for stochastic optimization,” *arXiv preprint arXiv:1412.6980*, 2014.
- [39] Y. LeCun, L. Jackel, L. Bottou, C. Cortes, J. S. Denker, H. Drucker, I. Guyon, U. Muller, E. Sackinger, P. Simard *et al.*, “Learning algorithms for classification: A comparison on handwritten digit recognition,” *Neural Networks*, vol. 261, p. 276, 1995.
- [40] J. Stallkamp, M. Schlipsing, J. Salmen, and C. Igel, “Man vs. computer: Benchmarking machine learning algorithms for traffic sign recognition,” *Neural Networks*, 2012.
- [41] A. Krizhevsky and G. Hinton, “Learning multiple layers of features from tiny images,” Tech. Rep., 2009.
- [42] K. He, X. Zhang, S. Ren, and J. Sun, “Deep residual learning for image recognition,” in *Proc. of CVPR*, 2016.
- [43] “https://www.cs.tau.ac.il/~wolf/ytfaces/,” YouTube Faces DB.
- [44] X. Chen, C. Liu, B. Li, K. Lu, and D. Song, “Targeted backdoor attacks on deep learning systems using data poisoning,” *arXiv preprint arXiv:1712.05526*, 2017.
- [45] Y. Sun, X. Wang, and X. Tang, “Deep learning face representation from predicting 10,000 classes,” in *Proc. of CVPR*, 2014.
- [46] O. Suciu, R. Mărginean, Y. Kaya, H. Daumé III, and T. Dumitraş, “When does machine learning fail? generalized transferability for evasion and poisoning attacks,” in *Proc. of USENIX Security*, 2018.
- [47] A. Demontis, M. Melis, M. Pintor, M. Jagielski, B. Biggio, A. Oprea, C. Nita-Rotaru, and F. Roli, “Why do adversarial attacks transfer? explaining transferability of evasion and poisoning attacks,” in *Proc. of USENIX Security*, 2019, pp. 321–338.
- [48] A. Chambolle, “An algorithm for total variation minimization and applications,” *Journal of Mathematical Imaging and Vision*, vol. 20, no. 1, pp. 89–97, 2004.

## APPENDIX

### A. Proof of Theorem 1 and 2

**Definition 3. Total variation distance [48].** For two probability distributions  $P_{X_1}$  and  $P_{X_2}$  on  $\mathcal{X}$ , the total variation distance between them is defined by

$$\|P_{X_1} - P_{X_2}\|_{TV} = \max_{C \subset \mathcal{X}} |P_{X_1}(C) - P_{X_2}(C)|.$$

**Definition 4.** Given  $\rho \in (0, 1)$ , two distributions  $X_1$  and  $X_2$  are called  $\rho$ -covert<sup>2</sup>, if  $\|X_1 - X_2\|_{TV} \leq \rho$ .

Because Theorem 1 assumes that  $\mathcal{X}_{trap} = \mathcal{X} = \mathcal{X}_{attack}$ , hence  $\rho = 0$ , the proof of Theorem 1 follows directly from that of Theorem 2.

<sup>2</sup>We use the total variation distance as it is a natural way to measure distances between distributions. Other notions of distance may also be applied.

TABLE IX  
MODEL ARCHITECTURE FOR MNIST. FC STANDS FOR FULLY-CONNECTED LAYER.

Layer Type	# of Channels	Filter Size	Stride	Activation
Conv	16	5×5	1	ReLU
MaxPool	16	2×2	2	-
Conv	32	5×5	1	ReLU
MaxPool	32	2×2	2	-
FC	512	-	-	ReLU
FC	10	-	-	Softmax

### Proof of Theorem 2.

*Proof.* After injecting the trapdoor  $\Delta$  into the model, we have  $\forall x \in \mathcal{X}_{trap}$ ,  $\Pr(\mathcal{F}_\theta(x + \Delta) = y_t \neq \mathcal{F}_\theta(x)) \geq 1 - \mu$ . Therefore, the partial gradient from  $x \in \mathcal{X}_{trap}$  towards  $x + \Delta$  becomes the major gradient to achieve the target  $y_t$ . That is,

$$\begin{aligned} & P_{x \in \mathcal{X}_{trap}} \left[ \frac{\partial[\ln g(x) - \ln g(x + \Delta)]}{\partial x} \geq \eta \right] \\ &= P_{x \in \mathcal{X}_{trap}} \left[ \frac{1}{g(x)} \frac{\partial g(x)}{\partial x} - \frac{1}{g(x + \Delta)} \frac{\partial g(x + \Delta)}{\partial x} \geq \eta \right] \\ &\geq 1 - \mu \end{aligned}$$

where  $\eta \in (0, 1)$ . Since  $\mathcal{X}_{trap}$  and  $\mathcal{X}_{attack}$  are  $\rho$ -covert, we have

$$\begin{aligned} & P_{x \in \mathcal{X}_{attack}} \left[ \frac{\partial[\ln g(x) - \ln g(x + \Delta)]}{\partial x} \geq \eta \right] \\ &\geq P_{x \in \mathcal{X}_{trap}} \left[ \frac{\partial[\ln g(x) - \ln g(x + \Delta)]}{\partial x} \geq \eta \right] - \rho \\ &\geq 1 - (\mu + \rho) \end{aligned}$$

We now compute the attack effectiveness via the major gradient:

$$\begin{aligned} & P_{x \in \mathcal{X}_{attack}} \left[ \frac{\partial[\ln g(x) - \ln g(x + \epsilon)]}{\partial x} \geq \eta \right] \\ &= P_{x \in \mathcal{X}_{attack}} \left[ \frac{1}{g(x)} \frac{\partial g(x)}{\partial x} - \frac{1}{g(x + \epsilon)} \frac{\partial g(x + \epsilon)}{\partial x} \geq \eta \right] \end{aligned}$$

If  $g(x + \epsilon) \approx g(x + \Delta)$ ,  $x \in \mathcal{X}_{attack}$ , we have

$$\begin{aligned} & P_{x \in \mathcal{X}_{attack}} \left[ \frac{\partial[\ln g(x) - \ln g(x + \epsilon)]}{\partial x} \geq \eta \right] \\ &\approx P_{x \in \mathcal{X}_{attack}} \left[ \frac{\partial[\ln g(x) - \ln g(x + \Delta)]}{\partial x} \geq \eta \right] \\ &\geq 1 - (\mu + \rho) \end{aligned}$$

□

Thus the attacker can launch  $(\mu + \rho, \mathcal{F}_\theta)$ -effective attack by moving the test sample along the trapdoor direction.

### B. Experiment Configuration

**Model Architecture.** We now present the architecture of DNN models used in our work.

- **MNIST** (Table IX) is a convolutional neural network (CNN) consisting of two pairs of convolutional layers connected by max pooling layers, followed by two fully connected layers.

TABLE X  
MODEL ARCHITECTURE OF GTSRB.

Layer Type	# of Channels	Filter Size	Stride	Activation
Conv	32	3×3	1	ReLU
Conv	32	3×3	1	ReLU
MaxPool	32	2×2	2	-
Conv	64	3×3	1	ReLU
Conv	64	3×3	1	ReLU
MaxPool	64	2×2	2	-
Conv	128	3×3	1	ReLU
Conv	128	3×3	1	ReLU
MaxPool	128	2×2	2	-
FC	512	-	-	ReLU
FC	43	-	-	Softmax

TABLE XI  
RESNET20 MODEL ARCHITECTURE FOR CIFAR10.

Layer Name (type)	# of Channels	Activation	Connected to
conv_1 (Conv)	16	ReLU	-
conv_2 (Conv)	16	ReLU	conv_1
conv_3 (Conv)	16	ReLU	pool_2
conv_4 (Conv)	16	ReLU	conv_3
conv_5 (Conv)	16	ReLU	conv_4
conv_6 (Conv)	16	ReLU	conv_5
conv_7 (Conv)	16	ReLU	conv_6
conv_8 (Conv)	32	ReLU	conv_7
conv_9 (Conv)	32	ReLU	conv_8
conv_10 (Conv)	32	ReLU	conv_9
conv_11 (Conv)	32	ReLU	conv_10
conv_12 (Conv)	32	ReLU	conv_11
conv_13 (Conv)	32	ReLU	conv_12
conv_14 (Conv)	32	ReLU	conv_13
conv_15 (Conv)	64	ReLU	conv_14
conv_16 (Conv)	64	ReLU	conv_15
conv_17 (Conv)	64	ReLU	conv_16
conv_18 (Conv)	64	ReLU	conv_17
conv_19 (Conv)	64	ReLU	conv_18
conv_20 (Conv)	64	ReLU	conv_19
conv_21 (Conv)	64	ReLU	conv_20
pool_1 (AvgPool)	-	-	conv_21
dropout_1 (Dropout)	-	-	pool_1
fc_ (FC)	-	Softmax	dropout_1

- **GTSRB** (Table X) is a CNN consisting of three pairs of convolutional layers connected by max pooling layers, followed by two fully connected layers.
- **YouTube Face** (Table XII) is the DeepID model trained on the YouTube Face dataset. It has three convolutional layers (connected by pooling layers) followed by three fully connected layers.
- **CIFAR10** (Table XI) is also a CNN but includes 21 sequential convolutional layers, followed by pooling, dropout, and fully connected layers.

**Detailed information on attack configuration.** We evaluate the trapdoor-enabled detection using six adversarial attacks: CW, ElasticNet, PGD, BPDA, SPSA, and FGSM (which we have described in Section II-A). Details about the attack configuration are listed in Table XIV.

**Sample Trapdoor Patterns.** Figure 11 shows sample images that contain a single-label defense trapdoor (a single  $6 \times 6$  square) and that contain an all-label defense trapdoor (five  $3 \times 3$  squares). The mask ratio of the trapdoors used in

TABLE XII  
DEEPIID MODEL ARCHITECTURE FOR YOUTUBE FACE.

Layer Name (Type)	# of Channels	Filter Size	Stride	Activation	Connected to
conv_1 (Conv)	20	4×4	2	ReLU	-
pool_1 (MaxPool)	-	2×2	2	-	conv_1
conv_2 (Conv)	40	3×3	2	ReLU	pool_1
pool_2 (MaxPool)	-	2×2	2	-	conv_2
conv_3 (Conv)	60	3×3	2	ReLU	pool_2
pool_3 (MaxPool)	-	2×2	2	-	conv_3
fc_1 (FC)	160	-	-	-	conv_3
conv_4 (Conv)	80	2×2	1	ReLU	pool_3
fc_2 (FC)	160	-	-	-	conv_4
add_1 (Add)	-	-	-	ReLU	fc_1, fc_2
fc_3 (FC)	1280	-	-	Softmax	add_1



(a) Single Label Defense Trapdoor (b) All Label Defense Trapdoor

Fig. 11. Sample trapdoor examples used in our defense. While the actual trapdoors we used all have a mask ratio of  $\kappa = 0.1$ , here we artificially increase  $\kappa$  from 0.1 to 1.0 in order to highlight the trapdoors from the rest of the image content.

our experiments is fixed to  $\kappa = 0.1$ .

**Datasets and Defense Configuration.** Table XIII lists the specific datasets and training process used to inject trapdoors into the four DNN models.

**Selecting Trapdoor Injection Ratio.** As mentioned earlier, our analysis shows that the size and diversity of the training data used to inject a trapdoor could affect its effectiveness of trapping attackers. To explore this factor, we define *trapdoor injection ratio* as the ratio between the trapdoored images and the clean images in the training dataset. Intuitively, a higher injection ratio should allow the model to learn the trapdoor better but could potentially degrade normal classification accuracy.

We defend the model with different trapdoor injection ratios and examine the detection success rate. We see that only when the injection ratio is very small (*e.g.*  $< 0.03$  for GTSRB), the model fails to learn the trapdoor and therefore detection fails. Otherwise the trapdoor is highly effective in terms of detecting adversarial examples. Thus when building the trapdoored models, we use an injection ratio of 0.1 for MNIST, GTSRB, CIFAR1010, and 0.01 for YouTube Face (see Table XIV).

### C. Additional Results on Comparing Trapdoor and Adversarial Perturbation

Figure 12 and Figure 13 show that the neuron signatures of adversarial inputs have high cosine similarity to the neuron signatures of trapdoors in a trapdoored CIFAR10 and YouTube

TABLE XIII  
 DETAILED INFORMATION ON DATASETS AND DEFENSE CONFIGURATIONS FOR EACH TRAPDOORED MODEL.

Model	# of Labels	Training Set Size	Testing Set Size	Per Label Injection Ratio	Mask Ratio	Training Configuration
MNIST	10	50,000	10,000	0.1	0.1	epochs=5, batch=32, optimizer=Adam, lr=0.001
GTSRB	43	35,288	12,630	0.1	0.1	epochs=30, batch=32, optimizer=Adam, lr=0.001
CIFAR10	10	50,000	10,000	0.1	0.1	epochs=100, batch=32, optimizer=Adam, lr=0.001
YouTube Face	1,283	375,645	64,150	0.01	0.1	epochs=30, batch=32, optimizer=Adadelata, lr=1

TABLE XIV  
 DETAILED INFORMATION ON ATTACK CONFIGURATIONS. FOR MNIST EXPERIMENTS, WE DIVID THE EPS VALUE BY 255.

Attack Method	Attack Configuration
CW	binary step size = 20, max iterations = 500, learning rate = 0.1, abort early = False
PGD	max eps = 8, # of iteration = 100, eps of each iteration = 1.0
ElasticNet	binary step size = 20, max iterations = 500, learning rate = 0.5, abort early = False
BPDA	max eps = 8, # of iteration = 100, eps of each iteration = 1.0
SPSA	eps = 8, # of iteration = 500, learning rate = 0.1
FGSM	eps = 8

Face models (left figures), and the trapdoor-free models (right figures).

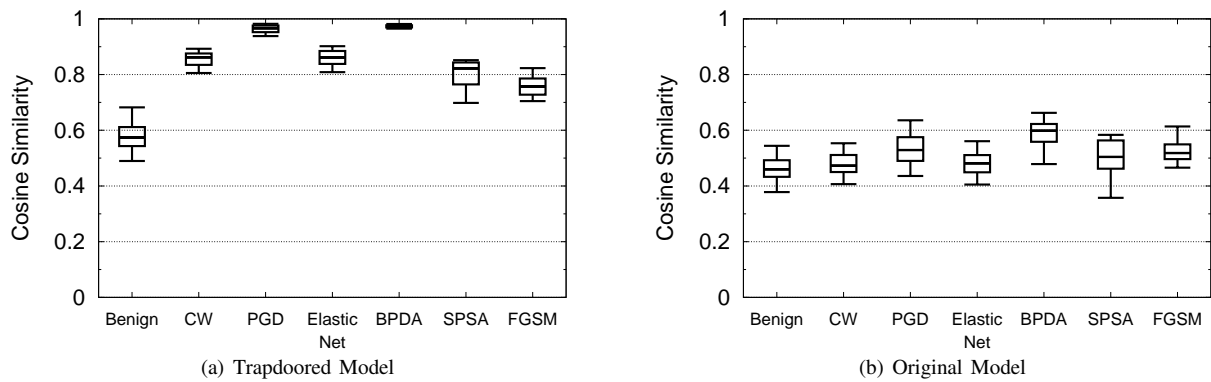


Fig. 12. Comparison of cosine similarity of normal images and adversarial images to trapdoored inputs in a trapdoored CIFAR10 model and in an original (trapdoor-free) CIFAR10 model. The boxes show the inter-quartile range, and the whiskers denote the 5<sup>th</sup> and 95<sup>th</sup> percentiles.

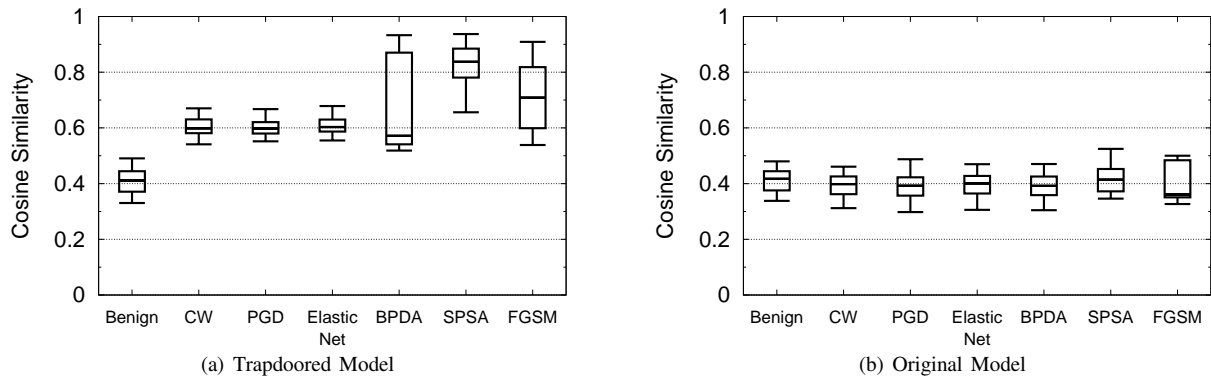


Fig. 13. Comparison of cosine similarity of normal images and adversarial images to trapdoored inputs in a trapdoored YouTube Face model and in an original (trapdoor-free) YouTube Face model. The boxes show the inter-quartile range, and the whiskers denote the 5<sup>th</sup> and 95<sup>th</sup> percentiles.